Finanziato dall'Unione europea NextGenerationEU
Ministero dell'Università e della Ricerca
Italiadomani PIANO NAZIONALE DI RIPRESA E RESILIENZA
Università degli Studi di Padova

Computational harmonic analysis on graphs

1. Calculating uncertainty principles on graphs

Wolfgang Erb

University of Padova

Workshop and Summer School on Applied Analysis 2024
September 16-20, 2024, Chemnitz, Germany

wolfgang.erb@unipd.it

Where is Padova (Padua)?

https://www.google.de/maps

General goal and outline of this presentation

Study of computational methods for harmonic analysis on graphs.

In the first part we will mainly treat uncertainty principles.

1. Introduction
   - An introduction to graph signal processing (GSP)
   - The graph Laplacian and the Graph Fourier Transform (GFT).
   - Graph Convolution
2. Uncertainty principles on graphs
   - Space and Frequency localization on graphs
   - Some particular uncertainty principles on graphs
   - How to calculate the shapes of uncertainty
   - Some applications in space-frequency analysis of signals

Why are graphs interesting?

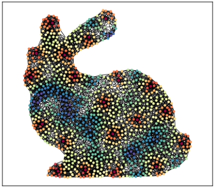 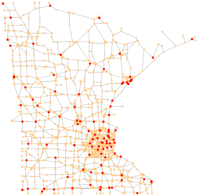 

Graphs offer the possibility to model complex irregular structures and relations inside these structures.

Examples:

- Social networks: nodes = persons, edges = relations
- Transport networks: nodes = cities, edges = streets
- Meshes: nodes = mesh nodes, edges = edges of triangulation

Graphs

We consider simple and undirected graphs G given as a triplet

$$G = (V, E, \mathbf{A}),$$

with vertices

$$V = \{\mathrm{v}_1, \ldots, \mathrm{v}_n\}$$

undirected edges $E \subset V \times V$ and a symmetric adjacency matrix $\mathbf{A} \in \mathbb{R}^{n \times n}$ with non-negative entries

$$\begin{cases} \mathbf{A}_{i,j} > 0 \text{ if } (\mathrm{v}_i, \mathrm{v}_j) \in E, \\ \mathbf{A}_{i,j} = 0 \text{ otherwise.} \end{cases}$$

Standard $\mathbf{A}$: only entries 1 (if there is an edge) and 0.
The degree matrix $\mathbf{D} \in \mathbb{R}^{n \times n}$ is the diagonal matrix with entries

$$\begin{cases} \mathbf{D}_{i,i} = \sum_{j=1}^{n} \mathbf{A}_{i,j} \\ \mathbf{D}_{i,j} = 0 \text{ if } i \neq j. \end{cases}$$

Labeled graph | Degree matrix $\mathbf{D}$ | Adjacency matrix $\mathbf{A}$

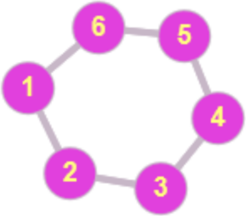

$$\begin{pmatrix} 2 & 0 & 0 & 0 & 0 & 0 \\ 0 & 2 & 0 & 0 & 0 & 0 \\ 0 & 0 & 2 & 0 & 0 & 0 \\ 0 & 0 & 0 & 2 & 0 & 0 \\ 0 & 0 & 0 & 0 & 2 & 0 \\ 0 & 0 & 0 & 0 & 0 & 2 \end{pmatrix} \quad \begin{pmatrix} 0 & 1 & 0 & 0 & 0 & 1 \\ 1 & 0 & 1 & 0 & 0 & 0 \\ 0 & 1 & 0 & 1 & 0 & 0 \\ 0 & 0 & 1 & 0 & 1 & 0 \\ 0 & 0 & 0 & 1 & 0 & 1 \\ 1 & 0 & 0 & 0 & 1 & 0 \end{pmatrix}$$

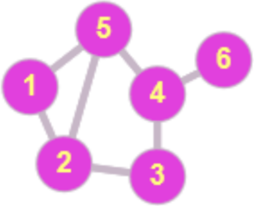

$$\begin{pmatrix} 2 & 0 & 0 & 0 & 0 & 0 \\ 0 & 3 & 0 & 0 & 0 & 0 \\ 0 & 0 & 2 & 0 & 0 & 0 \\ 0 & 0 & 0 & 3 & 0 & 0 \\ 0 & 0 & 0 & 0 & 3 & 0 \\ 0 & 0 & 0 & 0 & 0 & 1 \end{pmatrix} \quad \begin{pmatrix} 0 & 1 & 0 & 0 & 1 & 0 \\ 1 & 0 & 1 & 0 & 1 & 0 \\ 0 & 1 & 0 & 1 & 0 & 0 \\ 0 & 0 & 1 & 0 & 1 & 1 \\ 1 & 1 & 0 & 1 & 0 & 0 \\ 0 & 0 & 0 & 1 & 0 & 0 \end{pmatrix}$$

Graph signals

Graph signals are mappings $x : V \to \mathbb{R}$ (or $x : V \to \mathbb{C}$)

- A signal x is defined on the vertices $\mathrm{v} \in V$ of the graph
- We can represent x as a vector

$$x = (x(\mathrm{v}_1), \ldots, x(\mathrm{v}_n))^* \in \mathbb{R}^n \quad (\in \mathbb{C}^n).$$

- The linear space of all signals is denoted by $\mathcal{L}(G)$.

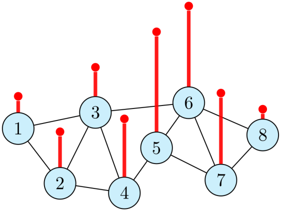

Fig.: Illustration of a graph signal x.

Graph signals

Example: brain connectivity networks:

- vertices: neural elements of the brain
- edges: pairwise relationships between elements
- graph signal: brain functional activity on vertices

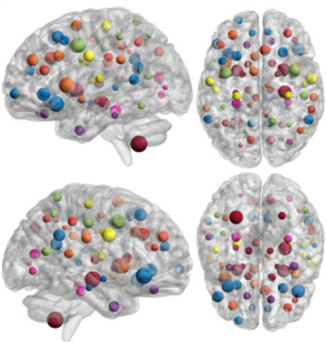

Fig.: Illustration of signals on a brain connectivity graph, Manjunatha et al. 2023

Graph signal processing (GSP)

In applications, graphs and graph signals might by huge. Necessity of efficient signal processing tools on graphs.

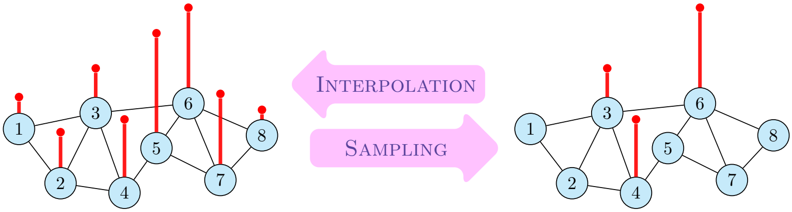

Goal of GSP: study of graph signals and possible processing tools

- Decomposition of signals (Fourier, wavelets, frames, etc.)
- Denoising of signals (convolution filters)
- Sampling and interpolation of signals
- $\underbrace{\text{Uncertainty principles}}_{\text{Main focus of this talk}}$

Graph Laplacian

Main ingredient for GSP is the graph Laplacian.

The graph Laplacian $\mathbf{L} \in \mathbb{R}^{n\times n}$ is defined as the matrix

$$\mathbf{L} = \mathbf{D} - \mathbf{A}, \quad \mathbf{L}_{i,j} := \begin{cases} \mathbf{D}_{i,i} & \text{if } i = j \\ -\mathbf{A}_{i,j} & \text{if } i \neq j \end{cases}.$$

The matrix $\mathbf{L}$ is symmetric and positive semi-definite.
$\dim(\ker \mathbf{L})$ is the number of connected components of G.

The normalized graph Laplacian $\mathbf{L}_N \in \mathbb{R}^{n\times n}$ is defined as

$$\mathbf{L}_N = \mathbf{D}^{-\frac{1}{2}} \mathbf{L} \mathbf{D}^{-\frac{1}{2}} = \mathbf{I}_n - \mathbf{D}^{-\frac{1}{2}} \mathbf{A} \mathbf{D}^{-\frac{1}{2}}.$$

The normalization ensures that the spectrum of $\mathbf{L}_N$ is in $[0, 2]$.

Labeled graph G

Graph Laplacian $\mathbf{L}$

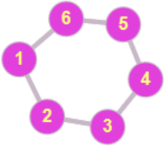

$$\begin{pmatrix} 2 & -1 & 0 & 0 & 0 & -1 \\ -1 & 2 & -1 & 0 & 0 & 0 \\ 0 & -1 & 2 & -1 & 0 & 0 \\ 0 & 0 & -1 & 2 & -1 & 0 \\ 0 & 0 & 0 & -1 & 2 & -1 \\ -1 & 0 & 0 & 0 & -1 & 2 \end{pmatrix}$$

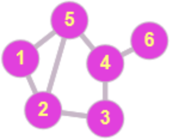

$$\begin{pmatrix} 2 & -1 & 0 & 0 & -1 & 0 \\ -1 & 3 & -1 & 0 & -1 & 0 \\ 0 & -1 & 2 & -1 & 0 & 0 \\ 0 & 0 & -1 & 3 & -1 & -1 \\ -1 & -1 & 0 & -1 & 3 & 0 \\ 0 & 0 & 0 & -1 & 0 & 1 \end{pmatrix}$$

Interpretation of the graph Laplacian

The graph Laplacian operates on a signal $x \in \mathcal{L}(G)$ as

$$\mathbf{L}x(\mathrm{v}_i) = \sum_{(\mathrm{v}_i,\mathrm{v}_j)\in E} \mathbf{A}_{i,j}(x(\mathrm{v}_i) - x(\mathrm{v}_j))$$

In many cases, $\mathbf{L}$ is a discretization of a continuous Laplacian

Example 1: the path graph P_n

Path graph P_n with n nodes and weights $\mathbf{A}_{i,j} = h^{-1}$.

Laplacian for P_n (interior nodes)

$$\mathbf{L}x(\mathrm{v}_i) = \frac{2x(\mathrm{v}_i) - x(\mathrm{v}_{i+1}) - x(\mathrm{v}_{i-1})}{h}$$

is a second order difference quotient that approximates $-\frac{\mathrm{d}^2 x}{\mathrm{d}t^2}(t)$.

Properties of the graph Laplacian

- $\mathbf{L}$ is symmetric (on undirected graphs).
- $\mathbf{L}$ is diagonally dominant, i.e. $\mathbf{L}_{i,i} \geq \sum_{j \neq i} |\mathbf{L}_{i,j}|$ for all i.
- We have

$$x^* \mathbf{L} x = \sum_{(i,j) \in E} \mathbf{A}_{i,j} (x_i - x_j)^2$$

  and therefore $x^* \mathbf{L} x \geq 0$ for all x. Thus, $\mathbf{L}$ is positive semi-definite.
- When $x \in \mathbb{R}^n$ represents a graph signal, $x^* \mathbf{L} x$ represents the energy of a discrete derivative (defined by the edges of the graph) and measures the smoothness of x.
- As $\mathbf{e}^* \mathbf{L} e = 0$, the constant signals are maximally smooth.
- Since $\mathbf{L} e = 0$, the graph Laplacian has at least one zero eigenvalue. If G is connected, $\mathbf{L}$ is of rank $n - 1$ (the kernel of $\mathbf{L}$ has dimension 1).

The Laplacian and the Fourier transform on graphs

Graph Fourier transform

Idea: use the orthonormal eigenvectors

$$\mathbf{L} u_k = \lambda_k u_k, \quad k \in \{1, \ldots, n\},$$

of the graph Laplacian $\mathbf{L}$ as Fourier basis and set

$$\hat{x}_k = \langle x, u_k \rangle = \sum_{i=1}^{n} x(\mathrm{v}_i) \overline{u_k(\mathrm{v}_i)}.$$

Note: $\mathbf{L}$ is symmetric, positive semi-definite. Thus, we can order the real eigenvalues as

$$0 = \lambda_1 \leq \lambda_2 \leq \cdots \leq \lambda_n.$$

The system $\{u_1, u_2, \ldots, u_n\}$ is an orthonormal basis of $\mathcal{L}(G)$.

Example 1: the path graph P_n

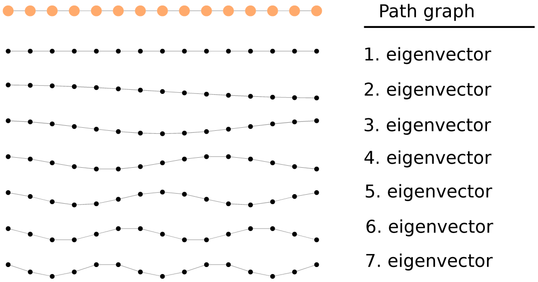

The eigenvalues and eigenfunctions can be written explicitly as

$$\lambda_k = 2 - 2\cos\left(\frac{(k-1)\pi}{n}\right)$$

and

$$u_1 = \frac{1}{\sqrt{n}}, \quad u_k(\mathrm{v}_i) = \sqrt{\frac{2}{n}}\cos\left(\frac{(k-1)\pi(i-0.5)}{n}\right), \; k \geq 2.$$

The graph Fourier transform corresponds in this case to the Discrete Cosine Transform (DCT II).

Example 2: the bunny graph

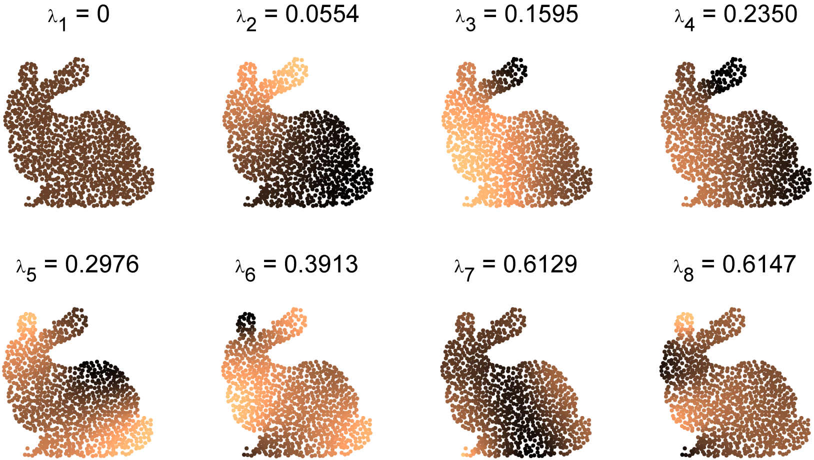

The first 8 eigenfunctions of the graph Laplacian $\mathbf{L}$ on the bunny graph.

Example 3: circle graphs

We consider the circle graph $C_n = \{1, \ldots, n\}$ with the set of edges given as

$$E = \{(i,j) \in C_n \times C_n : |i-j| = 1 \mod n\}.$$

In fact C_n can also be considered as a group (the cyclic group $\mathbb{Z}/n\mathbb{Z}$ with generating element 1.)
As adjacency matrix we have

$$\mathbf{A}_{i,j} = \begin{cases} 1 \text{ if } (i,j) \in E, \\ 0 \text{ otherwise.} \end{cases}$$

Cyclic group C_6

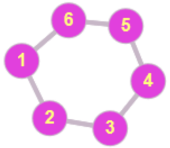

Graph Laplacian $\mathbf{L}$ of C_6

$$\begin{pmatrix} 2 & -1 & 0 & 0 & 0 & -1 \\ -1 & 2 & -1 & 0 & 0 & 0 \\ 0 & -1 & 2 & -1 & 0 & 0 \\ 0 & 0 & -1 & 2 & -1 & 0 \\ 0 & 0 & 0 & -1 & 2 & -1 \\ -1 & 0 & 0 & 0 & -1 & 2 \end{pmatrix}$$

Example 3: circle graphs

The graph Laplacian $\mathbf{L}$ of C_n is a circulant matrix and the normalized characters

$$u_k(i) = \frac{1}{\sqrt{n}} \exp\left(\frac{\imath 2\pi i k}{n}\right), \quad k \in \{1, \ldots, n\},$$

form a complete orthonormal eigenbasis of $\mathbf{L}$ with respect to the eigenvalues

$$\lambda_k = 2 - 2\cos\left(\frac{2\pi k}{n}\right).$$

The graph Fourier transform corresponds in this case to the discrete Fourier transform. Note that

$$\lambda_k = \lambda_{n-k},$$

i.e., for cyclic groups the eigenspaces of $\mathbf{L}$ are degenerate. In particular, also for general graphs G we can not expect to have unique basis elements u_k for the Fourier transform.

Interpretation of the graph Fourier transform

The GFT can be interpreted similarly as a classical Fourier transform.

- the eigenvalues of the Laplacians $\mathbf{L}$, $\mathbf{L}_N$, can be interpreted as frequencies, i.e., the larger the eigenvalue the higher the frequency of the respective eigenvector.
- The eigenvectors associated with large eigenvalues oscillate rapidly while the eigenvectors associated with small eigenvalues vary slowly.
- The eigenvector associated to the eigenvalue 0 is constant (for $\mathbf{L}$).

The Fourier transform $\hat{x} = (\hat{x}_1, \ldots, \hat{x}_n)^*$ can be interpreted as the decomposition of a graph signal x into its single frequency components

$$x(\mathrm{v}_i) = \sum_{k=1}^{n} \hat{x}_k u_k(\mathrm{v}_i).$$

- The lower frequencies compose smooth part of the signal.
- The higher frequencies build the noisy part of the signal.

Matrix formulation of the GFT

As the grah Laplacian $\mathbf{L}$ is symmetric and positive semi-definite, we can write its eigendecomposition as

$$\mathbf{L} = \mathbf{U}\mathbf{M}_\Lambda\mathbf{U}^*,$$

where $\mathbf{M}_\Lambda = \mathrm{diag}(\lambda_1, \ldots, \lambda_n)$ contains the eigenvalues of $\mathbf{L}$ (increasingly ordered) and the unitary matrix $\mathbf{U} = (u_1 \; u_2 \; \cdots \; u_n)$ the corresponding eigenvectors.

Then, we can write the Graph Fourier transform of x as

$$\hat{x} = \mathbf{U}^* x, \quad \text{with } k\text{-th. entry} \quad \hat{x}_k = u_k^* x = \langle x, u_k \rangle.$$

The inverse Fourier transform is correspondingly given as

$$x = \mathbf{U}\hat{x}.$$

Convolution on graphs

Convolution in $\mathbb{R}$

$$(x * y)(s) = \int_{\mathbb{R}} x(t)y(s-t)\mathrm{d}t.$$

In the Fourier domain:

$$\widehat{(x * y)}(\omega) = \hat{x}(\omega)\hat{y}(\omega)$$

Graph convolution

No translation available
Idea: define convolution via graph Fourier transform

$$\widehat{(x * y)}_k = \hat{x}_k \hat{y}_k$$

We define the graph convolution as

$$y * x := \mathbf{U}\mathbf{M}_{\hat{y}}\hat{x} = \mathbf{U}\mathbf{M}_{\hat{y}}\mathbf{U}^* x, \quad \text{where } \mathbf{M}_{\hat{y}} = \mathrm{diag}(\hat{y}_1, \ldots \hat{y}_n).$$

Further, we define the convolution matrix $\mathbf{C}_x \in \mathbb{R}^{n \times n}$ as

$$\mathbf{C}_y = \mathbf{U}\mathbf{M}_{\hat{y}}\mathbf{U}^*.$$

Note: the graph convolution depends on the choice of the basis u_k.

Application: denoising of graph signals

Question: how can we remove the noisy part of a signal?

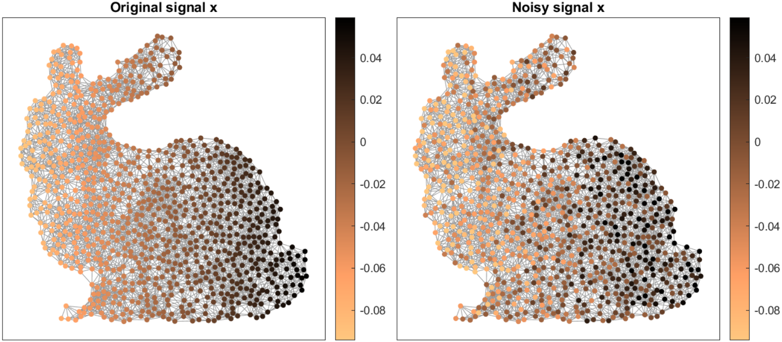

Figure 1: The original signal x and a noisy signal x_{noise} on the bunny graph.

Application: denoising of graph signals

To identify the noisy part of the signal x_{noise}, let's have a look at the Graph Fourier transform of x and x_{noise}.

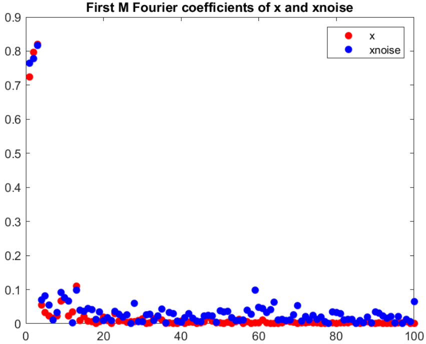

Figure 2: The size of the first 100 Fourier coefficients of the original signal x and the noisy signal x_{noise} on the bunny graph. We see that starting from $k \approx 15$, the frequency components $(\hat{x}_{\mathrm{noise}})_k$ are much larger than for $\hat{x}_k$.

Application: denoising of graph signals

Idea for the filter function y: generate y such that all frequencies $(\hat{x}_{\mathrm{noise}})_k$, $k \geq 21$, of x_{noise} are removed, i.e., calculate

$$x_{\mathrm{denoised}} = y * x_{\mathrm{noise}},$$

where y is a low-pass filter that cuts off all frequencies larger than $k = 20$.

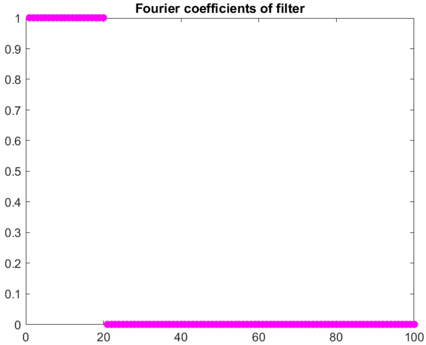

Figure 3: The Fourier coefficients of the low-pass filter y.

Application: denoising of graph signals

Result: denoised signal x_{denoised} calculated in terms of the Fourier coefficients

$$(\hat{x}_{\mathrm{denoised}})_k = \begin{cases} \hat{x}_k & \text{for } k \leq 20, \\ 0 & \text{for } k > 20. \end{cases}$$

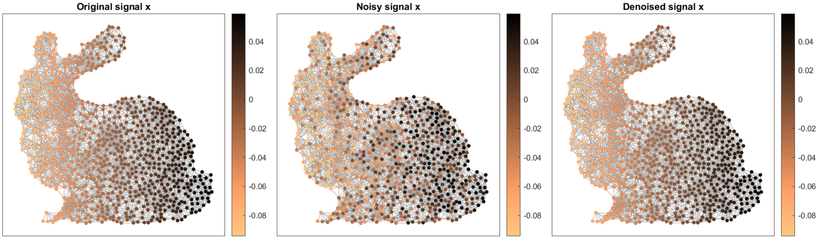

Figure 4: The original signal x, the noisy signal x_{noise} and the denoised x_{denoised}.

Uncertainty principles in harmonic analysis

Uncertainty principles describe the following phenomenon encountered in different settings of harmonic analysis:

"A function and its Fourier transform can not both be well-localized"

One famous examples is Heisenberg's uncertainty principle:

Theorem 1 (Heisenberg-Pauli-Weyl)

For any $f \in L^2(\mathbb{R})$ and any $a, b \in \mathbb{R}$, we have

$$\int_{\mathbb{R}} (t-a)^2 |f(t)|^2 \mathrm{d}t \int_{\mathbb{R}} (\omega - b)^2 |\hat{f}(\omega)|^2 \mathrm{d}\omega \geq \frac{\|f\|_2^4}{(4\pi)^2}$$

Equality holds if and only if $f(x) = Ce^{2\imath bt} e^{-\gamma(t-a)^2}$, with $C \in \mathbb{C}$, $\gamma > O$.

Normalizing f such that $\|f\|_2 = 1$, we can visualize this uncertainty as:

$$y = \left(\int_{\mathbb{R}} (\omega - b)^2 |\hat{f}(\omega)|^2 \mathrm{d}\omega \right)^{1/2}$$

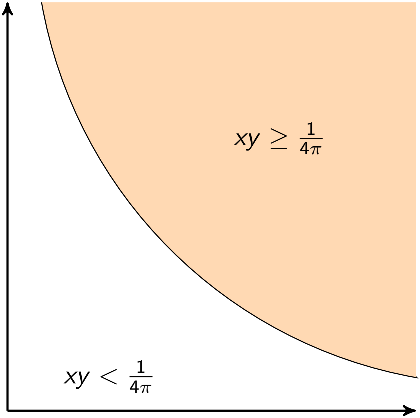

$$x = \left(\int_{\mathbb{R}} (t - a)^2 |f(t)|^2 \mathrm{d}t \right)^{1/2}$$

Landau-Pollak-Slepian uncertainty principle

Assume that $\|f\|_2 = 1$ and that the time and frequency localization of f in the intervals $[-a, a]$ and $[-b, b]$ is described through the values

$$\alpha^2 = \int_{-a}^{a} |f(t)|^2 \mathrm{d}t, \quad \beta^2 = \int_{-b}^{b} |\hat{f}(\omega)|^2 \mathrm{d}\omega.$$

Then the pairs (α, β) can attain only the following values in $[0, 1]^2$:

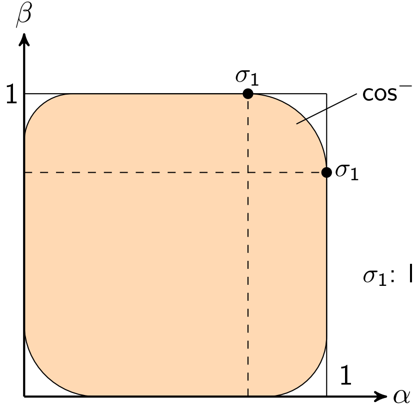

$\cos^{-1}\alpha + \cos^{-1}\beta \geq \cos^{-1}\sqrt{\sigma_1}$

σ_1: largest possible α for $\beta = 1$

Vertex-frequency localization on graphs

For a vertex-frequency analysis of a signal x on G we use spatial and spectral filter functions $f, g \in \mathbb{R}^n$ with the properties

$$0 \leq f \leq 1,\ 0 \leq \hat{g} \leq 1, \quad \text{and} \quad \|f\|_\infty = \|\hat{g}\|_\infty = 1. \tag{1}$$

Based on the filters f and g we introduce the localization operators

$$\begin{aligned} \mathbf{M}_f x &:= f\, x \quad \text{(pointwise product)}, \\ \mathbf{C}_g x &:= g * x = \mathbf{U}\mathbf{M}_{\hat{g}}\mathbf{U}^* x \quad \text{(graph convolution)}. \end{aligned}$$

- We call $\mathbf{M}_f$ with the filter f space localization operator;
- We call $\mathbf{C}_g$ with the filter g frequency localization operator;
- $\mathbf{M}_f$ and $\mathbf{C}_g$ are symmetric and positive semidefinite;
- $\mathbf{M}_f$ and $\mathbf{C}_g$ have spectral norm equal to 1.

Vertex-frequency localization on graphs

For $\mathbf{M}_f$ and $\mathbf{C}_g$ we define the expectation values

$$\bar{\mathbf{m}}_f(x) := \frac{\langle \mathbf{M}_f x, x \rangle}{\|x\|^2}, \qquad \bar{\mathbf{c}}_g(x) := \frac{\langle \mathbf{C}_g x, x \rangle}{\|x\|^2}.$$

- x is called space-localized with respect to f if $\bar{\mathbf{m}}_f(x)$ is close to one.
- x is called frequency-localized with respect to g if $\bar{\mathbf{c}}_g(x)$ approaches 1.

We define the set of admissible values related to $\mathbf{M}_f$ and $\mathbf{C}_g$ as

$$\mathcal{W}(\mathbf{M}_f, \mathbf{C}_g) := \left\{ (\bar{\mathbf{m}}_f(x), \bar{\mathbf{c}}_g(x)) \; : \; \|x\| = 1 \right\} \subset [0,1]^2. \tag{2}$$

We call $\mathcal{W}(\mathbf{M}_f, \mathbf{C}_g)$ the numerical range of the pair $(\mathbf{M}_f, \mathbf{C}_g)$. All studied uncertainty principles are linked to the boundaries of $\mathcal{W}(\mathbf{M}_f, \mathbf{C}_g)$.

Space-frequency operators

To investigate the joint localization with respect to both filters f and g and to describe the set $\mathcal{W}(\mathbf{M}_f, \mathbf{C}_g)$, we consider the two operators

$$\mathbf{R}_{f,g}^{(\theta)} := \cos(\theta)\,\mathbf{M}_f + \sin(\theta)\,\mathbf{C}_g \quad \text{and} \quad \mathbf{S}_{f,g} := \mathbf{C}_g^{1/2}\mathbf{M}_f\mathbf{C}_g^{1/2},$$

where $\mathbf{C}_g^{1/2}$ denotes the square root of the positive semidefinite $\mathbf{C}_g$.

- $\mathbf{R}_{f,g}^{(\theta)}$ as combination of $\mathbf{M}_f$ and $\mathbf{C}_g$ is symmetric for any $0 \leq \theta < 2\pi$.
- $\mathbf{S}_{f,g} \in \mathbb{R}^{n \times n}$ is a positive semi-definite with norm bounded by 1.

Space-frequency operators

Related to the operators $\mathbf{R}_{f,g}^{(\theta)}$, $\mathbf{S}_{f,g}$, we consider the expectation values:

$$\bar{\mathbf{r}}_{f,g}^{(\theta)}(x) := \frac{\langle \mathbf{R}_{f,g}^{(\theta)} x, x\rangle}{\|x\|^2} = \cos(\theta)\bar{\mathbf{m}}_f(x) + \sin(\theta)\bar{\mathbf{c}}_g(x),$$

$$\bar{\mathbf{s}}_{f,g}(x) := \frac{\langle \mathbf{S}_{f,g} x, x\rangle}{\|x\|^2}.$$

To formulate uncertainty principles, the largest eigenvalues $\rho_1^{(\theta)}$ and σ_1 and eigenvectors $\phi_1^{(\theta)}$ and ψ_1 are of major importance.

For σ_1, we have

$$\sigma_1 = \|\mathbf{S}_{f,g}\| = \|\mathbf{M}_f^{1/2}\mathbf{C}_g^{1/2}\|^2 = \|\mathbf{C}_g^{1/2}\mathbf{M}_f^{1/2}\|^2 = \|\mathbf{M}_f^{1/2}\mathbf{C}_g\mathbf{M}_f^{1/2}\|.$$

Example 1, projection-projection filters

Let $\chi_{\mathcal{A}}$ denote the indicator function of a set $\mathcal{A}$, i.e.

$$\chi_{\mathcal{A}}(\mathrm{v}) := \begin{cases} 1 & \text{if } \mathrm{v} \in \mathcal{A}, \\ 0 & \text{if } \mathrm{v} \notin \mathcal{A}. \end{cases}$$

For a subset $\mathcal{A}$ of the node set V and a subset $\mathcal{B}$ of the frequencies, we define the filter functions f and g as

$$f = \chi_{\mathcal{A}} \quad \hat{g} = \chi_{\mathcal{B}}. \tag{3}$$

- $\mathbf{M}_f$ and $\mathbf{C}_g$ are in this case orthogonal projectors satisfying

$$\mathbf{M}_f^2 = \mathbf{M}_f \quad \text{and} \quad \mathbf{C}_g^2 = \mathbf{C}_g.$$

- $\mathbf{S}_{f,g}$ is in this case equivalently given as $\mathbf{S}_{f,g} = \mathbf{C}_g \mathbf{M}_f \mathbf{C}_g$.

References:

- Studied by Landau, Pollak and Slepian in the 60's for signals on $\mathbb{R}$.
- General theory for projection operators in Hilbert spaces (Havin & Jöricke).
- Studied for graphs by Tsitsivero, Barbarossa, Di Lorenzo.

Example 2, distance-projection filters

Consider the geodesic distance $\mathrm{d}(\mathrm{v},\mathrm{w})$ on the graph. We set

$$\mathrm{d}_{\mathrm{w}}(\mathrm{v}) := \mathrm{d}(\mathrm{v},\mathrm{w}), \quad \mathrm{d}_{\mathrm{w}}^{\infty} := \max_{\mathrm{v}\in V} \mathrm{d}(\mathrm{v},\mathrm{w}).$$

Then, as spatial filter f and frequency filter g, we define

$$f(v) = 1 - \frac{\mathrm{d}_{\mathrm{w}}(\mathrm{v})}{\mathrm{d}_{\mathrm{w}}^{\infty}}, \quad \text{and} \quad \hat{g} = \chi_{\mathcal{B}}, \tag{4}$$

i.e., the spatial filter f incorporates the distance d_{w} to a reference node w. For this distance filter f we have

$$\mathbf{M}_f x = x - \tfrac{1}{\mathrm{d}_{\mathrm{w}}^{\infty}} \mathbf{M}_{\mathrm{d}_{\mathrm{w}}} x, \quad \bar{\mathbf{m}}_f(x) = 1 - \frac{x^* \mathbf{M}_{\mathrm{d}_{\mathrm{w}}} x}{\mathrm{d}_{\mathrm{w}}^{\infty} \|x\|^2}.$$

References:

- Similar distance-projection filters have been used also in a continuous setting on the real line and on the sphere (Erb, Mathias).

Example 3, Distance-Laplace filter

Another spectral filter $\hat{g} = (\hat{g}_1 \; \cdots \; \hat{g}_n)$ on $\hat{G}$ can be defined as

$$\hat{g}_j = 1 - \lambda_j/2, \tag{5}$$

where λ_j denotes the j-th. smallest eigenvalue of the graph Laplacian $\mathbf{L}$. In this case, we get

$$\mathbf{C}_g x = \mathbf{U}(\mathbf{I}_n - \tfrac{1}{2}\mathbf{M}_\lambda)\mathbf{U}^* x = (\mathbf{I}_n - \tfrac{1}{2}\mathbf{L})x.$$

Using a (modified) distance filter as a spatial filter, we get

$$\bar{\mathbf{m}}_f(x) = 1 - \frac{x^* \mathbf{M}_{\mathrm{d}_\mathrm{w}^2} x}{(\mathrm{d}_\mathrm{w}^\infty)^2 \|x\|^2}, \qquad \bar{\mathbf{c}}_g(x) = 1 - \frac{x^* \mathbf{L} x}{2\|x\|^2}.$$

References:

- Agaskar, Lu used such filters to obtain uncertainties on graphs based on spatial and spectral spreads.

Examples of spatial filters

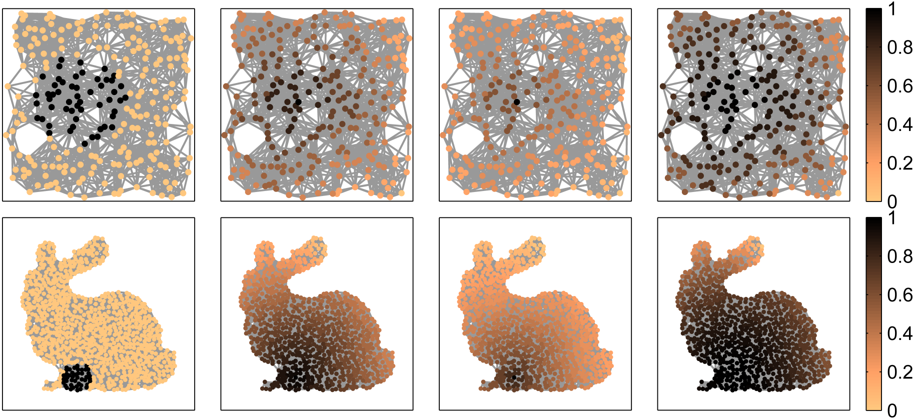

From left to right the following spatial filters:

$$f_1(\mathrm{v}) = \chi_{\mathcal{A}}(\mathrm{v}) \quad \text{(Example 1)}, \qquad f_2(\mathrm{v}) = 1 - \frac{\mathrm{d_w}(\mathrm{v})}{\mathrm{d_w^\infty}} \quad \text{(Example 2)},$$

$$f_3(\mathrm{v}) = 1 - \left(\frac{\mathrm{d_w}(\mathrm{v})}{\mathrm{d_w^\infty}}\right)^{\frac{1}{2}}, \qquad f_4(\mathrm{v}) = 1 - \left(\frac{\mathrm{d_w}(\mathrm{v})}{\mathrm{d_w^\infty}}\right)^{2} \quad \text{(Example 3)}.$$

Uncertainty principle related to the operator $\mathbf{S}_{f,g}$

Theorem 2

The range $\mathcal{W}(\mathbf{M}_f, \mathbf{C}_g)$ *is contained in the domain* $\mathcal{W}_\gamma^{(f,g)}$ *given by*

$$\mathcal{W}_\gamma^{(f,g)} = \left\{ (t,s) \in [0,1]^2 \;\middle|\; \begin{array}{ll} s \leq \gamma_{f,g}(t) & \text{if } ts \geq \sigma_1^{(f,g)}, \\ 1-s \leq \gamma_{f,g^*}(t) & \text{if } t(1-s) \geq \sigma_1^{(f,g^*)}, \\ s \leq \gamma_{f^*,g}(1-t) & \text{if } (1-t)s \geq \sigma_1^{(f^*,g)}, \\ 1-s \leq \gamma_{f^*,g^*}(1-t) & \text{if } (1-t)(1-s) \geq \sigma_1^{(f^*,g^*)} \end{array} \right\}$$

where $\sigma_1^{(f,g)}$ *is the largest eigenvalue of* $\mathbf{S}_{f,g}$,

$$\gamma_{f,g} : [\sigma_1^{(f,g)}, 1] \to \mathbb{R} : \quad \gamma_{f,g}(t) := \left((t\,\sigma_1^{(f,g)})^{\frac{1}{2}} + ((1-t)(1-\sigma_1^{(f,g)}))^{\frac{1}{2}} \right)^2.$$

and $f^* = 1-f$, $g^* = 1-g$.

Uncertainty principle related to the operator $\mathbf{S}_{f,g}$

Graphical version of Theorem 2.

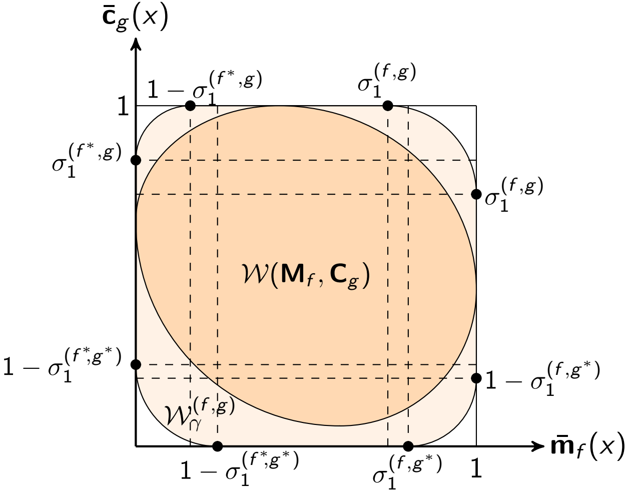

Note: If $\mathbf{M}_f$ and $\mathbf{C}_g$ are projectors, we have $\mathcal{W}(\mathbf{M}_f, \mathbf{C}_g) = \mathcal{W}_\gamma^{(f,g)}$.

Uncertainty principle related to the operator $\mathbf{R}_{f,g}^{(\theta)}$

Theorem 3

For every $0 \leq \theta < 2\pi$, *we have the inclusion*

$$\mathcal{W}(\mathbf{M}_f, \mathbf{C}_g) \subseteq [0,1]^2 \cap \mathcal{H}^{(\theta)},$$

with the half-plane

$$\mathcal{H}^{(\theta)} := \{(t,s) \mid \cos(\theta)\, t + \sin(\theta)\, s \leq \rho_1^{(\theta)}\}$$

having a supporting line $\mathcal{L}^{(\theta)}$ *that intersects the boundary of* $\mathcal{W}(\mathbf{M}_f, \mathbf{C}_g)$. *On the other hand, for every point* p *on the boundary of* $\mathcal{W}(\mathbf{M}_f, \mathbf{C}_g)$ *we have an angle* $0 \leq \theta < 2\pi$ *such that* $p \in \mathcal{L}^{(\theta)}$. *For this angle, we get an eigenvector* $\phi_1^{(\theta)}$ *(not necessarily unique) corresponding to the largest eigenvalue* $\rho_1^{(\theta)}$ *of* $\mathbf{R}_{f,g}^{(\theta)}$ *such that*

$$p = (\phi_1^{(\theta)*} \mathbf{M}_f \phi_1^{(\theta)}, \phi_1^{(\theta)*} \mathbf{C}_g \phi_1^{(\theta)}).$$

Uncertainty principle related to the operator $\mathbf{R}^{(\theta)}_{f,g}$

Graphical version of Theorem 3.

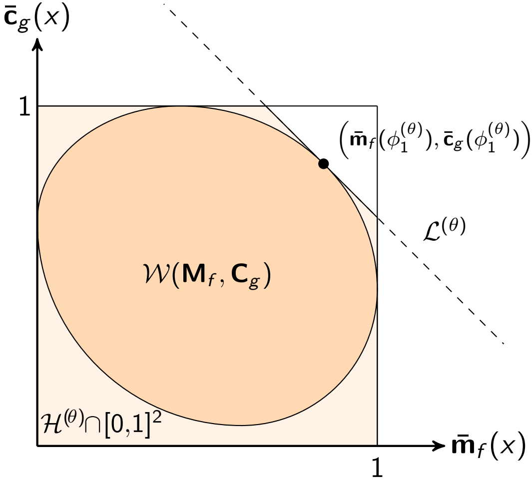

Note: for $n \geq 3$, the numerical range $\mathcal{W}(\mathbf{M}_f, \mathbf{C}_g)$ is convex.

Numerical calculation of $\mathcal{W}(\mathbf{M}_f, \mathbf{C}_g)$

Using a set $\Theta = \{\theta_1, \ldots \theta_K\} \subset [0, 2\pi)$ of $K \geq 3$ different angles, we approximate the numerical range $\mathcal{W}(\mathbf{M}_f, \mathbf{C}_g)$ with the two K-gons

$$\mathcal{P}_{\mathrm{out}}^{(\Theta)}(\mathbf{M}_f, \mathbf{C}_g) := \bigcap_{k=1}^{K} \mathcal{H}^{(\theta)} = \bigcap_{k=1}^{K} \left\{ (t,s) \mid \cos(\theta_k)\, t + \sin(\theta_k)\, s \leq \rho_1^{(\theta_k)} \right\},$$

$$\mathcal{P}_{\mathrm{in}}^{(\Theta)}(\mathbf{M}_f, \mathbf{C}_g) := \mathrm{conv}\{p^{(\theta_1)}, p^{(\theta_2)}, \ldots p^{(\theta_K)}\}.$$

The convexity of the numerical range $\mathcal{W}(\mathbf{M}_f, \mathbf{C}_g)$ (for $n \geq 3$) combined with the statements of Theorem 3 imply the following result.

Theorem 4

Let $\Theta = \{\theta_1, \ldots \theta_K\} \subset [0, 2\pi)$ be a set of $K \geq 3$ different angles and $n \geq 3$. Then,

$$\mathcal{P}_{\mathrm{in}}^{(\Theta)}(\mathbf{M}_f, \mathbf{C}_g) \subseteq \mathcal{W}(\mathbf{M}_f, \mathbf{C}_g) \subseteq \mathcal{P}_{\mathrm{out}}^{(\Theta)}(\mathbf{M}_f, \mathbf{C}_g).$$

Algorithm 1: Calculation of polygonal approximation to $\mathcal{W}(\mathbf{M}_f, \mathbf{C}_g)$

Input: $\mathbf{M}_f$, $\mathbf{C}_g$, angles $0 \leq \theta_1 < \theta_2 < \cdots < \theta_K < 2\pi$, with $K \geq 3$. Set $\theta_0 = \theta_K$.

for $k \in \{1, 2, \ldots, K\}$ **do**

Create $\mathbf{R}_{f,g}^{(\theta_k)} = \cos(\theta_k)\mathbf{M}_f + \sin(\theta_k)\mathbf{C}_g$;

Calculate norm. eigenvector $\phi_1^{(\theta_k)}$ for max. eigenvalue $\rho_1^{(\theta_k)}$;

Create boundary point $p^{(\theta_k)} = \left(\phi_1^{(\theta_k)*}\mathbf{M}_f\phi_1^{(\theta_k)}, \phi_1^{(\theta_k)*}\mathbf{C}_g\phi_1^{(\theta_k)}\right)$.

Generate interior polygon $\mathcal{P}_{\mathrm{in}}^{(\Theta)}(\mathbf{M}_f,\mathbf{C}_g) = \mathrm{conv}\{p^{(\theta_1)},\ldots,p^{(\theta_K)}\}$ to approximate $\mathcal{W}(\mathbf{M}_f, \mathbf{C}_g)$.

for $k \in \{1, 2, \ldots, K\}$ **do**

Create the outer vertex $q^{(\theta_k)}$.

Generate $\mathcal{P}_{\mathrm{out}}^{(\Theta)}(\mathbf{M}_f, \mathbf{C}_g) = \mathrm{conv}\{q^{(\theta_1)}, \ldots q^{(\theta_K)}\}$ as a polygon exterior to $\mathcal{W}(\mathbf{M}_f, \mathbf{C}_g)$.

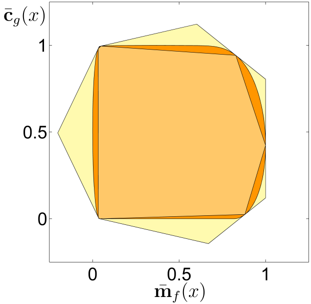

Fig.: Interior and exterior approximation of the numerical range $\mathcal{W}(\mathbf{M}_f, \mathbf{C}_g)$ based on Algorithm 1 with $K = 7$ vertices.

Shapes of uncertainty - illustrations

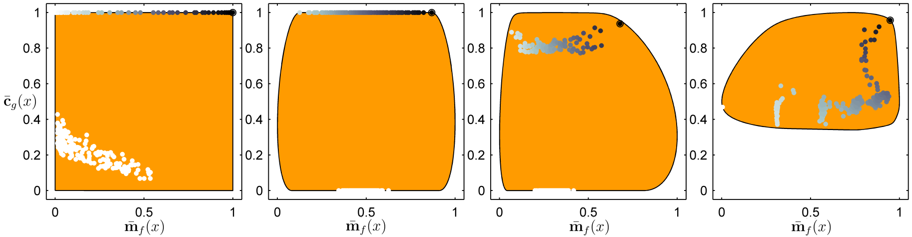

The numerical range $\mathcal{W}(\mathbf{M}_f, \mathbf{C}_g)$ for four filter pairs on the sensor network. The first, second and fourth plot correspond to the filters described in Example 1, 2 and 3.

The dots represent the position $(\bar{\mathbf{m}}_f(\psi_k), \bar{\mathbf{c}}_g(\psi_k))$ of the eigenvectors of the operator $\mathbf{S}_{f,g}$. The color (from black to white) of the dots indicates the corresponding eigenvalue σ_k (in the range from 1 to 0).

Shapes of uncertainty - illustrations

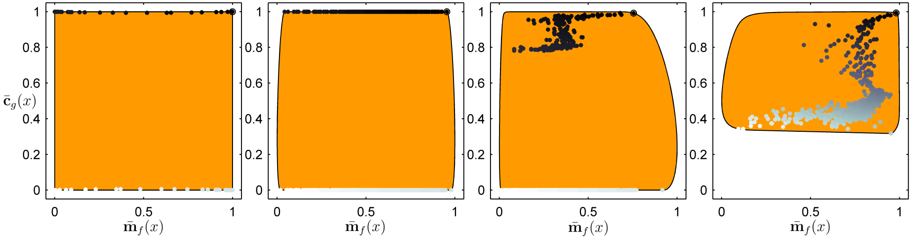

The numerical range $\mathcal{W}(\mathbf{M}_f, \mathbf{C}_g)$ for four filter pairs on the bunny network. The first, second and fourth plot correspond to the filters described in Example 1, 2 and 3.

The dots represent the position $(\bar{\mathbf{m}}_f(\psi_k), \bar{\mathbf{c}}_g(\psi_k))$ of the eigenvectors of the operator $\mathbf{R}_{f,g}^{(\theta)}$ with $\theta = 9\pi/20$. The color (from black to white) of the dots indicates the corresponding eigenvalue $\rho_k^{(\theta)}$ (in the range from 1 to 0).

Space-frequency localization of eigenvectors of $\mathbf{S}_{f,g}$, $\mathbf{R}_{f,g}^{(\theta)}$.

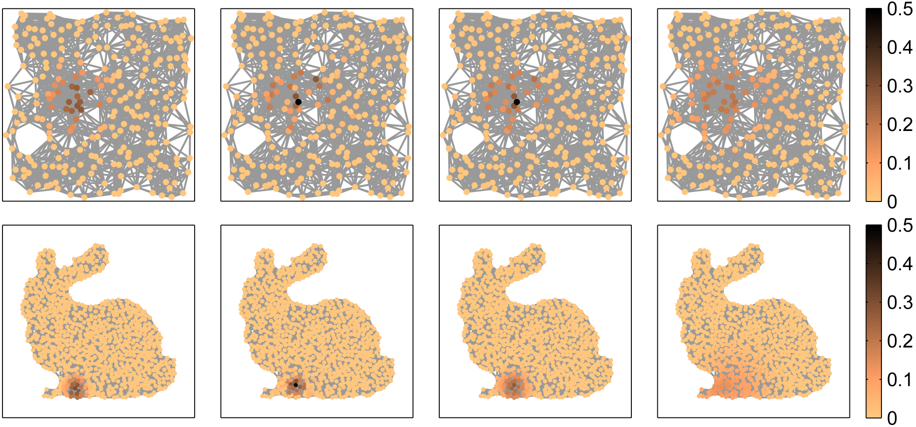

Top row: the eigenvector ψ_1 of the operator $\mathbf{S}_{f,g}$ for the sensor graph and four different filter pairs.

Bottom row: the eigenvector $\phi_1^{(\theta)}$ of the operator $\mathbf{R}_{f,g}^{(\theta)}$ with $\theta = \frac{9}{20}\pi$ for the bunny graph and four filter pairs.

Space-frequency localization of eigenvectors of $\mathbf{S}_{f,g}$.

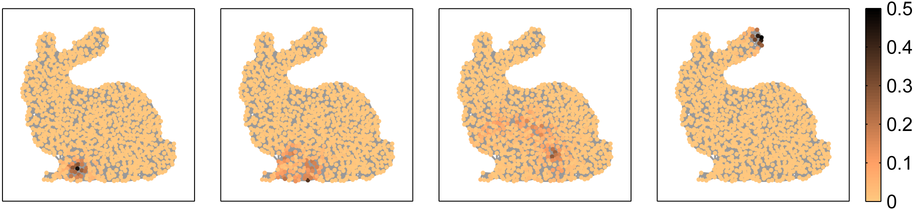

The eigenvectors ψ_1 ψ_{10}, ψ_{50} and ψ_{200} of $\mathbf{S}_{f,g}$ on the bunny graph for the distance-projection filter (Example 2).

Conclusion

Uncertainty relations are useful tool for the development of basis systems/dictionaries on graphs with prescribed space-frequency properties.

- $\mathbf{S}_{f,g}$ and $\mathbf{R}_{f,g}^{(\theta)}$ provide explicit uncertainty principles for graphs;
- The operator $\mathbf{R}_{f,g}^{(\theta)}$ can be used to calculate the shapes of the uncertainties (aka the numerical range $\mathcal{W}(\mathbf{M}_f, \mathbf{C}_g)$);
- The eigendecompositions of the operators $\mathbf{S}_{f,g}$ and $\mathbf{R}_{f,g}^{(\theta)}$ help to construct orthogonal basis systems with a space-frequency behavior determined by the operators $\mathbf{M}_f$ and $\mathbf{C}_g$;
- The shapes of the uncertainties provide useful information on the joint range of the localization operators $\mathbf{M}_f$ and $\mathbf{C}_g$ and on how complementary the two filters f and g are.

Thanks a lot for your attention!

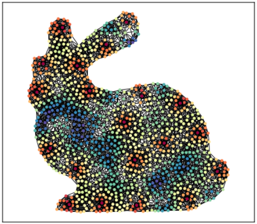

General introduction to Graph Signal Processing:

[1] ORTEGA, A. Introduction to Graph Signal Processing, *Cambridge University Press* (2022)

Article related to this talk:

[2] ERB, W. Shapes of Uncertainty in Spectral Graph Theory, *IEEE Trans. Inform. Theory 67:2* (2021), 1291-1307

Software to create the uncertainty shapes

https://github.com/WolfgangErb/GUPPY